Robust Adaptive Null Broadening Method Based on FDA-MIMO Radar

ZIHANG DING[ID], **JUNWEI XIE, BO WANG, AND HAOWEI ZHANG**[ID]
Air and Missile Defense College, Air Force Engineering University, Xi'an 710051, China

Corresponding author: Haowei Zhang (zhw_xhzf@163.com)

ABSTRACT Beamforming plays an important role in the array radar anti-interference. However, the interference targets with fast speed may move out of the narrow null area of the beampattern. A null broadening method with robust adaptive beamforming for frequency diverse array (FDA)-multiple-input and multiple-output (MIMO) systems is proposed in this paper. The projection preprocessing and windowing functions are applied to obtain stable beampatterns. Then, a novel null broadening method based on the covariance matrix reconstruction is realized by setting artificial fluctuations around each actual jammer. Finally, a new convex optimization model is established and solved to estimate the desired steering vector. Numerical simulations results verify the effectiveness of the proposed method.

INDEX TERMS Null broadening, frequency diverse array-multiple-input and multiple-output (FDA-MIMO), robust beamforming.

I. INTRODUCTION

The concept of frequency diverse array (FDA) was proposed in 2006 [1], [2]. The most important difference between FDA and a conventional phased-array (PA) is that a small frequency offset compared to the carrier frequency is used across the array elements, which results in a range-angle dependent beampattern [3]. Therefore, the FDA borings additional information in a certain range and provides more flexibility in system design and signal processing [4]–[6]. Recently, the multiple-input and multiple-output (MIMO) radar has attracted wide attention in recent years due to its promising advantages, such as the increased degrees-of-freedom (DoFs) and spatial diversity gain [7]. However, the beampattern of the traditional MIMO radar only depends on the angle and causes difficult in distinguishing targets and suppressing interferences located in the same direction but different ranges. As a result, a combination of the FDA with MIMO was proposed in [8], [9]. The advantages of the range-angle-dependent beampattern and increased DoFs are connected to realize the decoupling of range and angle. Hence, the FDA-MIMO systems can be employed for the unambiguous joint range and angle estimation, deceptive jamming suppression, and range ambiguous clutter suppression [9]–[13]. According to these

advantages, the FDA-MIMO can distinguish jamming targets at the same angle but different ranges.

The purpose of adaptive beamforming is to enhance the desired signal while simultaneously suppressing interference in the spatial domain. As for the FDA-MIMO, the adaptive beamforming with range-angle correlation can be formed [14]. However, in practice, the good performance of conventional adaptive beamforming is hard to achieve, especially when the interference is fluctuating. For example, some interference targets have fast speed, which will cause the interference targets moving out of the null areas. Moreover, the angle and range estimation on interference targets may have some errors which decreases the signal to interference plus noise ratio (SINR). A solution of keeping the interference in the null areas is broadening the null widths. In other words, a wider attenuation is formed in the area where the interference may appear to effectively suppress the interference direction fluctuation.

Null broadening technology has been extensively studied by transforming the sample covariance matrix [15]–[17]. A method to broaden the null widths based on the Capon spatial spectrum estimator was proposed in [18]. In [19], the covariance matrix was reconstructed by the obtained taper matrix and the sample covariance matrix. However, these methods have poor robustness against mismatches in the array. In ref. [20], a robust beamformer against fast-moving

interferences based on the minimum dispersion criterion was put forward. Robust wideband adaptive beamforming with null broadening and constant beamwidth via adding virtual interferers around original interferers was proposed in [21]. The projection and diagonal loading null broadening beamforming were proposed in [22], and the performance of this method depends on the accuracy of the steering vector. In [23], an algorithm was presented based on interference-plus-noise covariance matrix reconstruction by setting up several virtual interference sources around the interferences in the Capon spatial spectrum. However, as far as we know, there is no work considering the reconstruction of the covariance matrix with the expected signal.

In this paper, a null broadening algorithm with robust adaptive beamforming based on covariance matrix reconstruction is proposed. First, with the assumption of the weight vector being known, we adopt the projection preprocessing and windowing functions to form the stable beampatterns. At the low signal to noise ratio (SNR) case, an improved projection method is used to solve the beam energy scattering problem. Then, we set some artificial fluctuation around each actual jammer and reconstruct the covariance matrix. Next, the desired steering vector is estimated by solving a new convex optimization problem. Finally, the weight vector can be obtained according to the minimum variance distortionless response (MVDR) beamformer based on the reconstructed covariance matrix, the estimated steering vector of the desired signal, and the projection preprocessing.

The remaining sections are organized as follows. The data model of FDA-MIMO is briefly introduced in Section II. Section III presents the improved adaptive beamforming algorithm and the method of controlling null areas. Simulations and results are given in Section IV. Section V concludes this paper.

Notation: such as **a** represent vectors, and boldfaced uppercase letters, such as **A** denotes the matrix. The conjugate, transpose, and conjugate transpose of a matrix or a vector are denoted by $(\bullet)^*$, $(\bullet)^T$, $(\bullet)^H$, respectively. The symbol $\mathbb{C}$ denotes the complex space. $E\{\bullet\}$ denotes the mathematical expectation. diag $(\bullet)$ denotes the diagonal matrix and $\|\bullet\|$ denotes the two norms of the matrix.

II. DATA MODEL

Without loss of generality, we consider a monostatic FDA–MIMO radar system equipped with an M-element transmit arrays and N-element receive arrays, both of which are uniform linear arrays (ULAs). The carrier frequency increases linearly in every array with a small frequency increment Δf.

The baseband signals emitted by the different elements are mutually orthogonal. The emitted signal of ith element satisfies [9]

$$f_i(t) = s_i(t) e^{j2\pi[f_0+(i-1)\Delta f]t}, \quad 0 < t < T_p \quad (1)$$

where T_p is the radar pulse duration, $s_i(t)$ denotes the baseband waveform, and f_0 is the carrier frequency.

Under the assumption of the far-field target, the signal received by the jth receive element of FDA-MIMO based on K targets can be expressed as

$$r_j(t) = \sum_{k=1}^{K} \sum_{i=1}^{M} \mu_k f_i\left(t - \tau_{i,j}^k\right) \quad (2)$$

where μ_k is the path loss coefficient corresponding to the kth target, $\tau_{i,j}^k$ is the time delay from the transmit signal of the ith transmit element to the jth receive element passing through the kth target. $\tau_{i,j}^k$ can be expressed as

$$\tau_{i,j}^k = \frac{2r_k - d(i-1)\sin(\theta_k) - d(j-1)\sin(\theta_k)}{c} \quad (3)$$

where r_k is the range between radar and kth target, θ_k is the angle of the kth target, and c is the speed of the electromagnetic wave.

With the narrowband condition, the waveform can be approximated as $s\left(t - \tau_{i,j}^k\right) \approx s(t)$. Since all baseband signals are orthogonal to each other and normalized, we have [9]

$$\int_{T_p} f_m(t) f_n^*(t - \tau) dt = \begin{cases} 0, & m \neq n \\ 1, & m = n, \end{cases} \quad \forall \tau \quad (4)$$

where τ denotes the time shift. After matched filtering, the transmit waveforms are separated. By stacking the filtered outputs of N receive elements, the guidance vector of the receive signal and can be obtained as

$$\mathbf{a}(\theta_k, r_k) = \boldsymbol{b}(\theta_k) \otimes \mathbf{a}_t(\theta_k, r_k) \quad (5)$$

where $\mathbf{a}_t(\theta_k, r_k) \in \mathbb{C}^{M \times 1}$ represents the range-angle dependent transmit steering vector and it can be written as

$$\mathbf{a}_t(\theta_k, r_k)$$
$$= \left[1, e^{j2\pi\left(\frac{d}{\lambda}\sin\theta_k - \frac{2\Delta fR_k}{c}\right)}, \cdots, e^{-j2\pi\left(\frac{d}{\lambda}\sin\theta_k - \frac{2\Delta fR_k}{c}\right)}\right]^T \quad (6)$$

$\boldsymbol{b}(\theta_k) \in \mathbb{C}^{N \times 1}$ represents the angle-dependent transmit steering vector and it can be expressed as

$$\mathbf{b}(\theta_k) = \left[1, e^{j2\pi\frac{d}{\lambda}\sin(\theta_k)}, \cdots, e^{j2\pi\frac{(N-1)d}{\lambda}\sin(\theta_k)}\right]^T \quad (7)$$

where L is the number of snapshots. The number of desired targets and interference targets is 1 and K respectively. The array sample data at the lth snapshot can be modeled as

$$\mathbf{x}(l) = \mathbf{x}_s(l)\mathbf{a}(\theta_s, r_s) + \sum_{k=1}^{K} \mathbf{x}_{in}(l)\mathbf{a}(\theta_k, r_k) + \mathbf{n}(l) \quad (8)$$

where $\mathbf{x}_s(l)\mathbf{a}(\theta_s, r_s)$, $\sum_{k=1}^{K}\mathbf{x}_{in}(l)\mathbf{a}(\theta_k, r_k)$, $\mathbf{n}(l)$ are the desired signal, interference signal, and additive white Gaussian noise vector, respectively. Moreover, $\theta_s, r_s, \theta_k, r_k$ can be estimated by the parameter estimation methods of FDA-MIMO radar. The covariance matrix cannot be accurately estimated in the practice, and the covariance matrix is often

replaced by the sample covariance matrix, which can be written as

$$\mathbf{R}_{s+in} = \frac{1}{L} \sum_{l=1}^{L} \mathbf{x}(l) \mathbf{x}^H(l) \qquad (9)$$

The output of the adaptive beamformer can be expressed as

$$y(l) = \mathbf{w}^H(\theta, r) \mathbf{x}(l) \qquad (10)$$

where $\mathbf{w}(\theta, r)$ denotes the $MN \times 1$ weight vector. The optimal beamformer can be obtained by solving the following problem with the MVDR criterion

$$\min_{\mathbf{w}} \mathbf{w}^H \mathbf{R}_{s+in} \mathbf{w}$$
$$\text{s.t. } \mathbf{w}^H \mathbf{a}(\theta_s, r_s) = 1$$

Hence, the optimal weight vector can be written as

$$\mathbf{w}_{opt} = \frac{\mathbf{R}_{s+in}^{-1} \mathbf{a}(\theta_s, r_s)}{\mathbf{a}^H(\theta_s, r_s) \mathbf{R}_{s+in}^{-1} \mathbf{a}(\theta_s, r_s)} = \mu \mathbf{R}_{s+in}^{-1} \mathbf{a}(\theta_s, r_s) \qquad (11)$$

If the desired signal can be separated from the interference signal, only the covariance matrix of the interference signal is needed to construct the weight vector. The optimal weight vector can be expressed as follows

$$\hat{\mathbf{w}}_{opt} = \frac{\mathbf{R}_{in}^{-1} \mathbf{a}(\theta_s, r_s)}{\mathbf{a}^H(\theta_s, r_s) \mathbf{R}_{in}^{-1} \mathbf{a}(\theta_s, r_s)} \qquad (12)$$

Although the weight vector constructed from interference signals alone has better performance than one constructed from expected and interference signals, it has some limitations. The desired signals and interference signals are usually mixed and are difficult to distinguish. Therefore, how to improve the effectiveness of the adaptive beam becomes important.

III. IMPROVED ADAPTIVE BEAMFORMING ALGORITHM

In this section, we discuss the method about how to improve the effectiveness of the adaptive beamforming and broaden null. In the sequel, we propose a processing method based on projection, windowing function, and a designing adaptive null broadening designing algorithm.

A. PROCESSING METHOD BASED ON PROJECTION WINDOWING

By eigenvalue decomposition, $\mathbf{R}_{s+in}$ can be transformed into the signal space and the noise space

$$\mathbf{R}_{s+in} = \mathbf{U}_s \mathbf{\Lambda}_s \mathbf{U}_s^H + \mathbf{U}_N \mathbf{\Lambda}_N \mathbf{U}_N^H \qquad (13)$$

The eigenvalues in the descending order are $\lambda_1, \lambda_2, \cdots, \lambda_{MN}$ and the corresponding eigenvectors are $\mathbf{u}_1, \mathbf{u}_2, \cdots, \mathbf{u}_{MN}$. Then, $\mathbf{w}_{opt}$ can be obtained by (11).

$$\tilde{\mathbf{w}}_{opt} = \mathbf{U}_s \mathbf{U}_s^H \mathbf{w}_{opt} \qquad (14)$$

However, when the input SNR is low that $\lambda_{K+1} \leq \lambda_{K+2}$, $\mathbf{U}_s$ can be updated as

$$\tilde{\mathbf{U}}_s = [\mathbf{u}_1, \cdots, \mathbf{u}_K, \mathbf{a}(\theta_s, r_s)] \qquad (15)$$

The complexity of the MVDR algorithm is mainly from the calculation of the covariance matrix, the eigenvalue decomposition and the inverse of the covariance matrix, whose complexity is $\mathcal{O}\{(MN)^2 L\}$, $\mathcal{O}\{(MN)^3\}$, $\mathcal{O}\{(MN)^3\}$, respectively. Thus, the complexity of the conventional and improved MVDR algorithm is $\mathcal{O}\{(MN)^2 L + (MN)^3\}$ and $\mathcal{O}\{(MN)^2 L + 2(MN)^3\}$, respectively. As the cost of superior performance, the complexity is increased compared with the traditional method.

To solve the high sidelobe problem, window function can be used, and the weight vector after adding windows can be written as

$$\widehat{\mathbf{w}}_{opt} = \mathbf{h}_w \odot \mathbf{U}_s \mathbf{U}_s^H \mathbf{w}_{opt} = \mathbf{h}_w \odot \tilde{\mathbf{w}}_{opt} \qquad (16)$$

B. THE PROPOSED ALGORITHM OF NULL BROADENING

We propose an algorithm of null broadening through the left and right rotation of the interference steering vector. The fluctuation values on the left and right sides in angle are $a\Delta\theta$, $b\Delta\theta$, respectively. $c\Delta r$, $d\Delta r$ denotes the values of the left and right sides in range, respectively. Due to $\Delta\theta \approx 0$, $\sin(\theta + \Delta\theta) \approx \sin\theta + \Delta\theta \cos\theta$ can be obtained. The fluctuation steering vector is then expressed as

$$\mathbf{z}_t(\Delta\theta, \Delta r)$$
$$= \left[1 \ e^{j2\pi\left(\frac{d\Delta\theta\cos\theta}{\lambda} - \frac{\Delta f \Delta r}{c}\right)} \cdots e^{j2\pi(M-1)\left(\frac{d\Delta\theta\cos\theta}{\lambda} - \frac{\Delta f \Delta r}{c}\right)} \right]^T \qquad (17)$$

The interference steering vector after left and right rotations can be respectively expressed as

$$\mathbf{a}(\theta_s - a\Delta\theta, r_s - c\Delta r) = \mathbf{B}_l \mathbf{a}(\theta_s, r_s) \qquad (18)$$

and

$$\mathbf{a}(\theta_s + b\Delta\theta, r_s + d\Delta r) = \mathbf{B}_r \mathbf{a}(\theta_s, r_s) \qquad (19)$$

where

$$\mathbf{B}_l = \text{diag}(\mathbf{b}(-a\Delta\theta) \otimes \mathbf{z}_t(-a\Delta\theta, -c\Delta r)) \qquad (20)$$

and

$$\mathbf{B}_r = \text{diag}(\mathbf{b}(b\Delta\theta) \otimes \mathbf{z}_t(b\Delta\theta, d\Delta r)) \qquad (21)$$

The covariance matrix after left and right rotations can be written as

$$\mathbf{R}_l = \mathbf{B}_l \mathbf{R}_{s+in} \mathbf{B}_l^H \qquad (22)$$

and

$$\mathbf{R}_r = \mathbf{B}_r \mathbf{R}_{s+in} \mathbf{B}_r^H \qquad (23)$$

respectively. The mean value of the covariance matrix is obtained as

$$\mathbf{R} = \frac{\mathbf{R}_l + \mathbf{R}_r}{2} \qquad (24)$$

The covariance matrix is brought into the process of solving the optimal weight vector, and the updated weight vector is obtained. When the null field needs to be expanded widely,

we can increase the number and values of left and right rotations and get the covariance matrix such as $\mathbf{R}_{l1}\mathbf{R}_{l2}$, $\mathbf{R}_{r1}$, $\mathbf{R}_{r2}$ … Then. calculate the mean value of these covariance matrixes.

$$\mathbf{R} = \frac{\sum_{p=1}^{P}\left(\mathbf{R}_{lp}+\mathbf{R}_{rp}\right)}{2P} \qquad (25)$$

where P denotes the number of fluctuations. In practice, the values of $\Delta\theta$, Δr are chosen artificially and the values are related to the accuracy in estimating interference angle, distance, and velocity.

C. DESIRED SIGNAL STEERING VECTOR ESTIMATION
When there are steering vector errors in the array, the performance loss mainly occurs brought by the mismatch of the steering vector, which may cause beam deviation to a certain extent. An accurate steering vector is needed to ensure the stability of the beam direction. To obtain the desired weight vector, an optimal method is proposed in this section.

The interference and noise space under the steering vector mismatch can be expressed as

$$\mathbf{I} - \frac{\tilde{\mathbf{a}}\tilde{a}^{\mathrm{H}}}{\tilde{\mathbf{a}}^{\mathrm{H}}\tilde{\mathbf{a}}}$$

The desired steering vector is projected into space and the first constraint is established as

$$\left\|\left(\mathbf{I} - \frac{\tilde{\mathbf{a}}\tilde{\mathbf{a}}^{\mathrm{H}}}{\tilde{\mathbf{a}}^{\mathrm{H}}\tilde{\mathbf{a}}}\right)\mathbf{a}\right\|^2 <\eta$$

where η denotes a positive number.

Compared with the Capon algorithm, the multiple signal classification (MUSIC) algorithm possesses higher accuracy in the target parameter estimation performance. The spectral density function is written as

$$P_{MUSIC} = \frac{1}{\mathbf{a}_x^{\mathrm{H}}(\theta_k, R_k)\,\mathbf{U}_N\mathbf{U}_N^{\mathrm{H}}\mathbf{a}_x(\theta_k, R_k)} \qquad (26)$$

According to the power spectrum, the second constraint is established as

$$\mathbf{a}^{\mathrm{H}}\mathbf{U}_N\mathbf{U}_N^{\mathrm{H}}\mathbf{a} < \tilde{\mathbf{a}}^{\mathrm{H}}\mathbf{U}_N\mathbf{U}_N^{\mathrm{H}}\tilde{\mathbf{a}} \qquad (27)$$

Therefore, the optimization problem can be written as

$$\min_a \quad \mathbf{a}^{\mathrm{H}}\mathbf{U}_N\mathbf{U}_N^{\mathrm{H}}\mathbf{a}$$
$$\text{s.t.} \quad \left\|\left(\mathbf{I} - \frac{\tilde{\mathbf{a}}\tilde{\mathbf{a}}^{\mathrm{H}}}{\tilde{\mathbf{a}}^{\mathrm{H}}\tilde{\mathbf{a}}}\right)\mathbf{a}\right\|^2 <\eta$$
$$\mathbf{a}^{\mathrm{H}}\mathbf{U}_N\mathbf{U}_N^{\mathrm{H}}\mathbf{a} < \tilde{\mathbf{a}}^{\mathrm{H}}\mathbf{U}_N\mathbf{U}_N^{\mathrm{H}}\tilde{\mathbf{a}} \qquad (28)$$

By solving the optimization problem, the desired signal steering vector will be obtained. Set $\Psi = \mathbf{I} - \frac{\tilde{\mathbf{a}}\tilde{\mathbf{a}}^{\mathrm{H}}}{\tilde{\mathbf{a}}^{\mathrm{H}}\tilde{\mathbf{a}}}$, and $\Gamma = \tilde{\mathbf{a}}\mathbf{U}_N\mathbf{U}_N^{\mathrm{H}}\tilde{\mathbf{a}}$, the Lagrange function can be expressed as

$$L(\mathbf{a}, \lambda_1, \lambda_2) = \mathbf{a}^{\mathrm{H}}\mathbf{U}_N\mathbf{U}_N^{\mathrm{H}}\mathbf{a} + \lambda_1\left(\mathbf{a}^{\mathrm{H}}\Psi\mathbf{a} - \eta\right)$$
$$+ \lambda_2\left(\mathbf{a}\mathbf{U}_N\mathbf{U}_N^{\mathrm{H}}\mathbf{a} - \Gamma\right) \qquad (29)$$

TABLE 1. Flow diagrams of algorithm.

step	Specific algorithm content
Step1	According to the algorithm of parameter estimation, the angle and range of target and jamming signal are estimated
Step2	The covariance matrixes $\mathbf{R}$ can be restructured by (25). The number of fluctuations denotes the width of the field
Step3	By solving the optimization problem (28), obtain the desired guide vector $\mathbf{a}$
Step4	Calculate the weight vector $\mathbf{w}_{opt}$ by (14) or (16)

Then, we can obtain

$$\frac{dL}{d\mathbf{a}} = 2\mathbf{U}_N\mathbf{U}_N^{\mathrm{H}}\mathbf{a} + 2\lambda_1\Psi\mathbf{a} + 2\lambda_2\mathbf{U}_N\mathbf{U}_N^{\mathrm{H}}\mathbf{a} = 0 \quad (30)$$
$$\frac{dL}{d\lambda_1} = \mathbf{a}^{\mathrm{H}}\Psi\mathbf{a} - \eta = 0$$

By solving the above equation, we can get $\mathbf{a}$. In addition, this optimization problem can be solved by the convex optimization toolbox (CVX). So far, both the weight vector and the reconstructed covariance matrix have been designed. The steps of solving the weight vector are summarized as Table 1.

IV. SIMULATION RESULT
In this section, simulations are performed to verify the effectiveness of the proposed method. The transmit and receive ULAs consisting of $M = 10$ and $N = 10$ elements with spacing being half a wavelength are considered. The output SINR can be obtained by $SINR = \frac{\mathbf{w}_{opt}^{\mathrm{H}}\mathbf{R}_s\mathbf{w}_{opt}}{\mathbf{w}_{opt}^{\mathrm{H}}\mathbf{R}_{in}\mathbf{w}_{opt}}$.

A. PERFORMANCE OF WEIGHT VECTOR WITHOUT NULL BROADENING
Assumed that the desired signal with fixed 10 dB SNR comes from $(0°, 20\text{km})$, and one interference signal with fixed 30 dB INR comes from the direction $(0°, 8.1 \text{ km})$. Set the number of snapshots $L = 500$ and the frequency increment $\Delta f = 4 \text{ kHz}$.
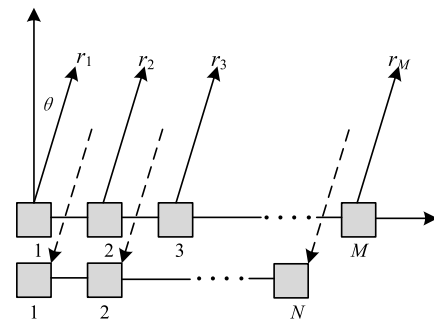

FIGURE 1. The model of sin-FDA-MIMO.

Fig.2 illustrates the adaptive beampattern obtained by different beamforming methods. From Fig. 2 (a) and (b), we can find that the beam energy is highly defocused and cannot form a stable main lobe. Fig.2 (c) and (d) show a stable beampattern in angle and range dimensions, which is obtained by (14). By comparison with Fig. 2 (a) and (c), the beampattern by projection preprocessing has better beam energy aggregation
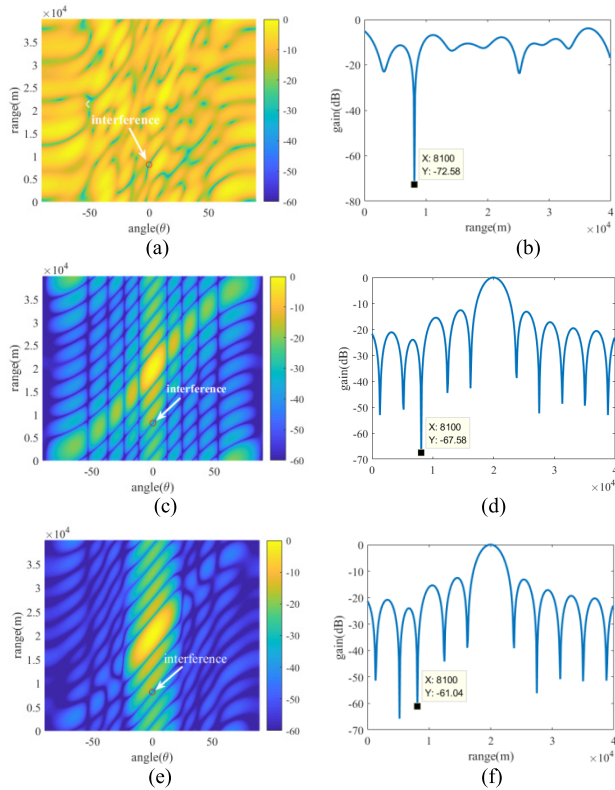
FIGURE 2. Beampatterns with an interference target. (a) 3-D beampattern with the conventional method. (b)2-D beampattern with the conventional method. (c) 3-D beampattern with the projection method. (d)2-D beampattern with the conventional method. (e) 3-D beampattern with the window. (f) 2-D beampattern with the window.
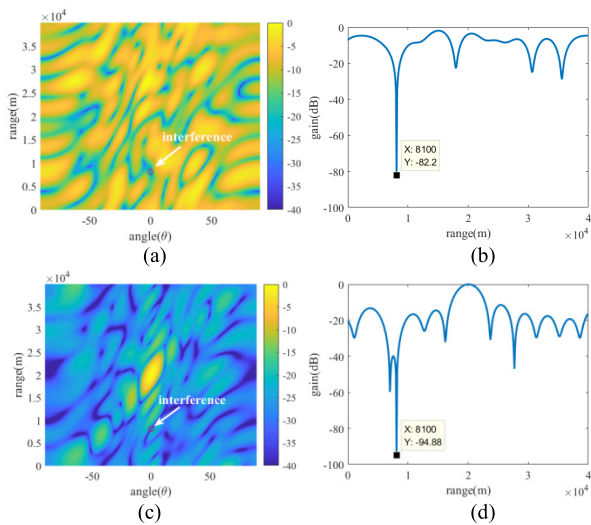

FIGURE 3. Beampatterns with low SNR. (a) 3-D beampattern with the projection method. (b) 2-D beampattern with the projection method. (c) 3-D beampattern with the improved projection method. (d) 2-D beampattern with the improved projection method.

FIGURE 4. Beampattern with two broadened null regions. (a) 3-D beampattern with the proposed method. (b) 2-D beampattern with different methods. (b) Output SINR versus input SNR.

and a more stable main lobe peak at the desired target position. The beampattern after adding Chebyshev windows is shown in Fig. 2(e) and (f). It is shown that the side lobe is decreased but the width of the main lobe is extended.
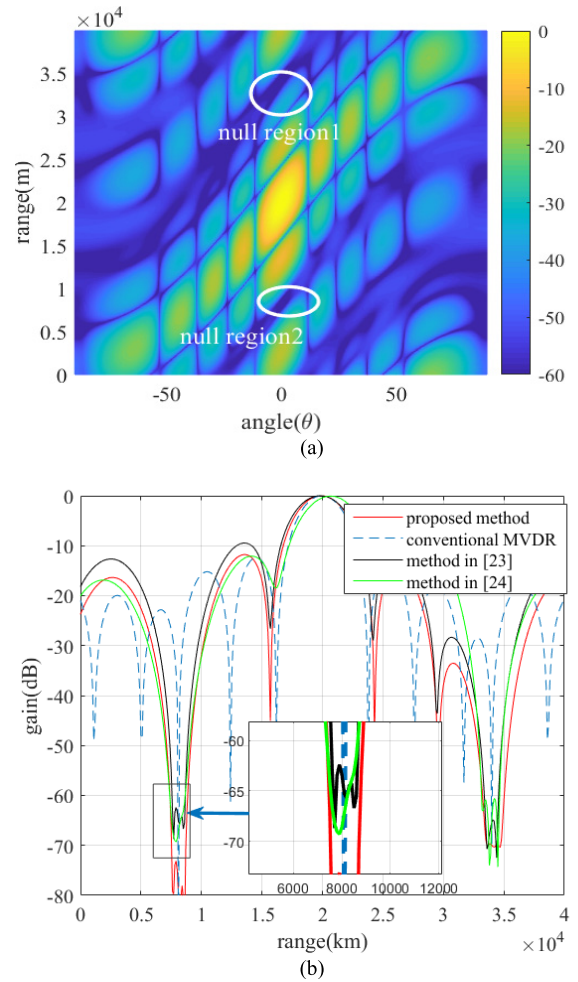
Changing the SNR to -30dB, the adaptive beampattern obtained by (14) is shown in Fig. 3 (a), and the 2-D adaptive beampattern obtained by (15) is illustrated in Fig.3(b). From Fig. 3, we can see that the improved projection preprocessing algorithm can obtain a better beam shape at the low SNR case.

B. PERFORMANCE OF NULL BROADENING METHOD

In this example, the beampatterns of null broadening are examined. Assumed that the desired signal comes from the $(0°, 20$ km$)$ with SNR $= 10$dB and two interference targets come from $(0°, 8.1$ km$)$, $(0°, 34$ km$)$ respectively with INR $= 40$dB. The area of the left and right rotations is located at $(\pm 0.5°, \pm 500$ m$)$. To simplify the calculation, set $a = b$, $c = d$. In the simulations, the proposed algorithm is compared with the following methods: (1) the covariance matrix reconstruction [23], (2) a linear constrained sector suppressed (LCSS) minimum power distortionless response (MPDR) beamformer [24].

Fig. 4 demonstrates that null broadening is achieved by the proposed method successfully. In addition, the proposed algorithm is compared with other methods in Fig. 4 (b) (c). As shown in Fig. 4 (a), the 3-D adaptive beampattern with multiple broadened null areas is obtained and the proposed null broadening method can widen the main lobe. The 2-D beampattern in distance dimension is shown in Fig. 4 (b), where the proposed and two other methods all effectively form null broadening. However, the null depths and widths of the proposed method significantly outperform the two other algorithms. To better compare the effect of null broadened, we calculate the output SINR versus input SNR of the three methods and show it in Fig. 4 (c). We can find that the output SNR of the proposed method is superior to the other two methods.

To compare the effect of fluctuation values on the null area, the beampattern with the different fluctuation values $(\Delta \theta, \Delta r)$ is examined in Fig. 5. The values $(\Delta \theta, \Delta r)$ are assumed to be $(0.5°, 200$ m$)$, and $(1°, 500$ m$)$. We can observe that the big value of $\Delta \theta$, Δr can obtain the wider null area apparently than the small value.
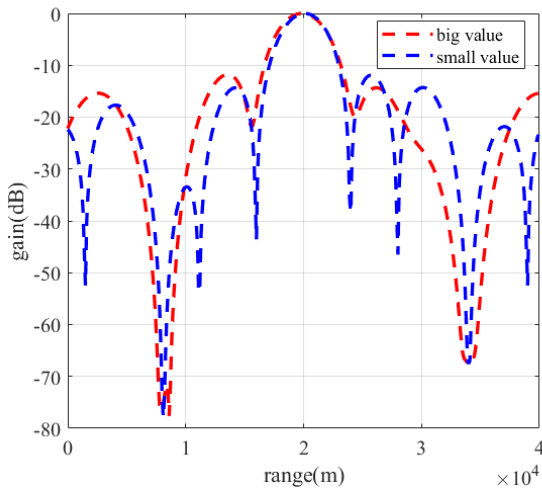

FIGURE 5. 2-D beampattern with different values of $\Delta \theta$, Δr.

C. PERFORMANCE OF DESIRED SIGNAL STEERING VECTOR ESTIMATION

In the third example, we examine the performance of the desired signal steering vector estimation. Assume that the

desired signal comes from $(0°, 20$ km$)$. The 2-D beampattern in distance dimension is shown in Fig.6, from which we can see that conventional adaptive beampattern cannot be formed in the desired signal direction when there is a steering vector mismatch, but the proposed algorithm can form a stable beampattern in the desired position.
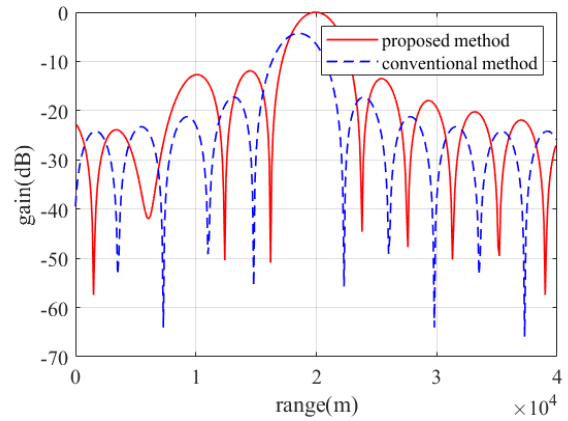

FIGURE 6. Beampattern with errors in the steering vector.
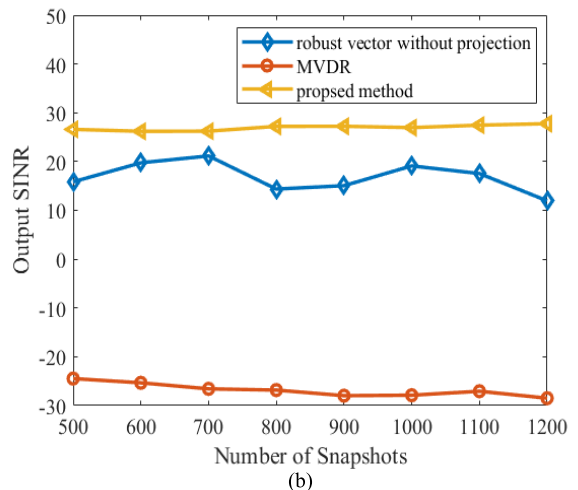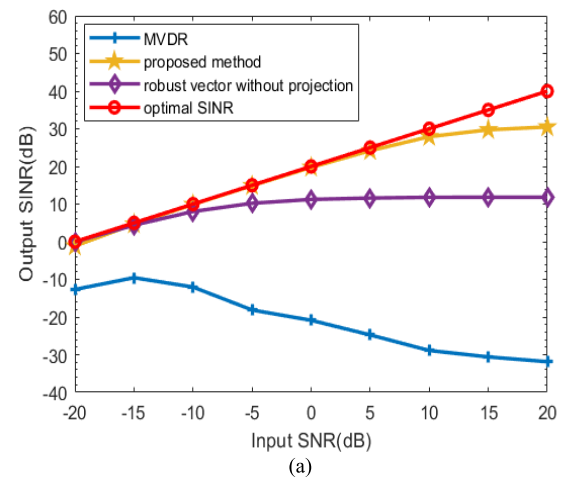

FIGURE 7. Performance against the steering vector error. (a) Output SINR versus input SNR. (b) Output SINR versus the number of snapshots.

The output SINR is utilized to evaluate the performance of the desired signal steering vector estimation. Fig.7 (a) shows the output SINR of these methods versus the input SNR. It can be seen that the performance of the proposed method is better than that of the other beamformers and is close to the optimal SINR. As shown in Fig.7 (b), the number of snapshots had no obvious effect on the performance of all beamformers. Therefore, the proposed method shows better performance than the other methods against the mismatch of the steering vector.

V. CONCLUSION

In this paper, a robust adaptive beampattern with accurately controlled null areas was proposed for the FDA–MIMO radar. The simulation results show that the improved projection method outperforms conventional methods and can obtain stable performance in the beamforming at the low SNR case. The width of the null areas can be controlled by adjusting the number and values of left and right rotations besides the depth of the null area is not lost and our proposed null broadening method can obtain higher SINR performance than the other two methods. Moreover, the optimization problem of estimating the desired steering vector can achieve good robustness against the errors caused by fast-moving jammers or antenna platform motion.

REFERENCES

[1] P. Antonik, M. C. Wicks, H. D. Griffiths, and C. J. Baker, "Frequency diverse array radars," in *Proc. IEEE Conf. Radar*, Verona, NY, USA, Apr. 2006, pp. 215–217.

[2] M. C. Wicks and P. Antonik, "Frequency diverse array with independent modulation of frequency, amplitude, and phase," U.S. Patent 7 319 427, Jan. 15, 2008.

[3] W. Khan, I. M. Qureshi, and S. Saeed, "Frequency diverse array radar with logarithmically increasing frequency offset," *IEEE Antennas Wireless Propag. Lett.*, vol. 14, pp. 499–502, 2015.

[4] K. Gao, W.-Q. Wang, H. Chen, and J. Cai, "Transmit beamspace design for multi-carrier frequency diverse array sensor," *IEEE Sensors J.*, vol. 16, no. 14, pp. 5709–5714, Jul. 2016.

[5] W. T. Li, C. Cui, X. T. Ye, X. W. Shi, and H. C. So, "Quasi-Time-Invariant 3-D focusing beampattern synthesis for conformal frequency diverse array," *IEEE Trans. Antennas Propag.*, vol. 68, no. 4, pp. 2684–2697, Apr. 2020.

[6] C. Wen, C. Ma, J. Peng, and J. Wu, "Bistatic FDA-MIMO radar space-time adaptive processing," *Signal Process.*, vol. 163, pp. 201–212, Oct. 2019.

[7] M. Akcakaya and A. Nehorai, "MIMO radar sensitivity analysis for target detection," *IEEE Trans. Signal Process.*, vol. 59, no. 7, pp. 3241–3250, Jul. 2011.

[8] P. F. Sammartino, C. J. Baker, and H. D. Griffiths, "Frequency diverse MIMO techniques for radar," *IEEE Trans. Aerosp. Electron. Syst.*, vol. 49, no. 1, pp. 201–222, Jan. 2013.

[9] J. Xu, G. Liao, S. Zhu, L. Huang, and H. C. So, "Joint range and angle estimation using MIMO radar with frequency diverse array," *IEEE Trans. Signal Process.*, vol. 63, no. 13, pp. 3396–3410, Jul. 2015.

[10] J. Xu, G. Liao, S. Zhu, and H. C. So, "Deceptive jamming suppression with frequency diverse MIMO radar," *Signal Process.*, vol. 113, pp. 9–17, Aug. 2015.

[11] Y. Yan, J. Cai, and W.-Q. Wang, "Two-stage ESPRIT for unambiguous angle and range estimation in FDA-MIMO radar," *Digit. Signal Process.*, vol. 92, pp. 151–165, Sep. 2019.

[12] F. L. Liu, X. P. Wang, M. X. Huang, L. T. Wan, H. F. Wang, and B. Zhang, "A novel unitary ESPRIT algorithm for monostatic FDA-MIMO radar," *Sensors*, vol. 20, no. 3, p. 827, 2020.

[13] W.-Q. Wang, H. Shao, and J. Cai, "Range-angle-dependent beamforming by frequency diverse array antenna," *Int. J. Antennas Propag.*, vol. 2012, Aug. 2012, Art. no. 760489.

[14] W.-Q. Wang, "Phased-MIMO radar with frequency diversity for range-dependent beamforming," *IEEE Sensors J.*, vol. 13, no. 4, pp. 1320–1328, Apr. 2013.

[15] R. J. Mailloux, "Covariance matrix augmentation to produce adaptive array pattern troughs," *Electron. Lett.*, vol. 31, no. 10, pp. 771–772, May 1995.

[16] M. Zatman, "Production of adaptive array troughs by dispersion synthesis," *Electron. Lett.*, vol. 31, no. 25, pp. 2141–2142, Dec. 1995.

[17] M. Zatman and J. R. Guerci, "Comments on 'Theory and application of covariance matrix tapers for robust adaptive beamforming' [with reply]," *IEEE Trans. Signal Process.*, vol. 48, no. 6, pp. 1796–1800, Jun. 2000.

[18] Y. Gu and A. Leshem, "Robust adaptive beamforming based on interference covariance matrix reconstruction and steering vector estimation," *IEEE Trans. Signal Process.*, vol. 60, no. 7, pp. 3881–3885, Jul. 2012.

[19] X. P. Yang, S. Li, T. Long, and T. K. Sarkar, "Adaptive null broadening method in wideband beamforming for rapidly moving interference suppression," *Electron. Lett.*, vol. 54, no. 16, pp. 1003–1005, Aug. 2018.

[20] L. Zhang, B. Li, L. Huang, T. Kirubarajan, and H. C. So, "Robust minimum dispersion distortionless response beamforming against fast-moving interferences," *Signal Process.*, vol. 140, pp. 190–197, Nov. 2017.

[21] X. Yang, S. Li, Y. Sun, T. Long, and T. K. Sarkar, "Robust wideband adaptive beamforming with null broadening and constant beamwidth," *IEEE Trans. Antennas Propag.*, vol. 67, no. 8, pp. 5380–5389, Aug. 2019.

[22] X. Mao, W. Li, Y. Li, Y. Sun, and Z. Zhai, "Robust adaptive beamforming against signal steering vector mismatch and jammer motion," *Int. J. Antennas Propag.*, vol. 2015, Jul. 2015, Art. no. 780296.

[23] J. Yang, J. Lu, X. Liu, and G. Liao, "Robust null broadening beamforming based on covariance matrix reconstruction via virtual interference sources," *Sensors*, vol. 20, no. 7, p. 1865, Mar. 2020.

[24] A. Amar and M. A. Doron, "A linearly constrained minimum variance beamformer with a pre-specified suppression level over a pre-defined broad null sector," *Signal Process.*, vol. 109, pp. 165–171, Apr. 2015.

ZIHANG DING was born in 1997. He received the bachelor's degree from the Air and Missile Defense College, Air Force Engineering University, Xi'an, Shaanxi, China, in 2019, where he is currently pursuing the master's degree. His research interests include beamforming and parameter estimation based on frequency diverse array radar.

JUNWEI XIE was born in 1970. He received the bachelor's, master's, and Ph.D. degrees from the Air and Missile Defense College, Air Force Engineering University, Xi'an, Shaanxi, China, in 1993, 1996, and 2009, respectively. He is currently a Professor with Air Force Engineering University. He has published more than 100 refereed journal articles, book chapters, and conference papers. His research interests include novel radar systems and jamming and anti-jamming.

BO WANG was born in 1991. He received the bachelor's and master's degrees from the Air and Missile Defense College, Air Force Engineering University, in 2013 and 2015, respectively. He is currently pursuing the Ph.D. degree with the Air and Missile Defense College. His research interests include signal processing and interference suppression technology based on FDA array radar.

HAOWEI ZHANG was born in 1992. He received the bachelor's, master's, and Ph.D. degrees from the Air and Missile Defense College, Air Force Engineering University, Xi'an, Shaanxi, China, in 2014, 2016, and 2020, respectively. He is currently a Lecturer with the Air and Missile Defense College. His research interests include multifunction radar resource management and intelligent scheduling.

. . .